Journal of Molecular Structure 933 (2009) 53–62

Contents lists available at ScienceDirect

Journal of Molecular Structure

journal homepage: www.elsevier.com/locate/molstruc

Crystal structures and temperature-induced phase transitions of $Sr_2Mn^{2+}W^{6+}O_6$, and of its transformation to $Sr_2Mn^{3+}W^{6+}O_{6+\delta}$

A. Faik [a,*], J.M. Igartua [a], G.J. Cuello [a,b], F. Jiménez-Villacorta [c,d], G.R. Castro [c,d], L. Lezama [e]

[a] Fisika Aplikatua II Saila, Zientzia eta Teknologia Fakultatea, UPV/EHU, PB 644, Bilbao 48080, Spain
[b] Ikerbasque and Institut, Laue Langevin, BP 156, F-38042 Grenoble, France
[c] SpLine Spanish CRG Beamline at the European Synchrotron Radiation Facilities, ESRF-BP 220-38043, Grenoble Cedex, France
[d] Instituto de Ciencia, de Materiales de Madrid (ICMM-CSIC), Cantoblanco, E-28049 Madrid, Spain
[e] Departamento de Química Inorgánica, Facultad de Ciencia y Tecnología, UPV/EHU, PB 644, Bilbao 48080, Spain

ARTICLE INFO

Article history:
Received 6 April 2009
Received in revised form 29 May 2009
Accepted 1 June 2009
Available online 12 June 2009

Keywords:
Double Perovskite
X-ray diffraction
Crystal structure
Phase transitions

ABSTRACT

We present a new effective method for synthesizing Sr_2MWO_6 double perovskite oxides: the co-precipitation route at 1220 K in nitrogen environment. Using conventional X-ray diffraction methods, we have confirmed the room-temperature space group of $Sr_2Mn^{2+}WO_6$ to be $P2_1/n$: $Z = 2$; $a = 5.6764(1)$Å; $b = 5.6752(1)$Å; $c = 8.0144(1)$Å; $\beta = 90.12(1)^\circ$ and $V = 258.18(1)$Å^3. We show that the compound presents the following temperature induced phase-transition sequence: $P2_1/n \rightarrow I4/m \rightarrow Fm\bar{3}m$. After a thermal treatment, 24 h at 870 K in air, the $Sr_2Mn^{2+}WO_6$ compound transforms irreversibly to $Sr_2Mn^{3+}WO_{6+\delta}$. This transformation has been confirmed by EPR and XANES measurements. Using conventional X-ray diffraction methods, we have shown the room-temperature space group of $Sr_2Mn^{3+}WO_{6+\delta}$ to be $I4/m$: $Z = 2$; $a = 5.6353(1)$ Å; $c = 8.0149(1)$ Å and $V = 254.53(1)$ Å^3. We show that the compound presents the following temperature induced phase-transition sequence: $I4/m(\rightarrow I4/mmm) \rightarrow Fm\bar{3}m$. The tetragonal-to-tetragonal phase transition is suggested to be present, it is not observed as it is very weak; it is attributed to the presence of the Jahn-Teller active Mn^{3+} cation.

1. Introduction

In the recent years compounds with general formula $A_2BB'O_6$ and double perovskite structure have been extensively studied. This attention is due to the fact that many compounds of this family present interesting electrical and magnetic properties that could be used in technological applications [1,2]. However, the structural properties of these materials have been relatively less studied. The double perovskite structure can be represented as a three-dimensional network of alternating BO_6 and $B'O_6$ octahedra, with A-atoms occupying the interstitial spaces. This structure is rather simple; but, the real crystal structure is sometimes difficult to determine, due to the pseudo-cubic symmetry, and due to the relative B-cation disorder that is present in many double perovskite compounds. Another difficulty has to do with the fact that single crystals of these materials have rarely been grown [3,4]. And, thus, most of the structural information has been obtained from powder diffraction data: conventional X-ray and neutrons. The study of the structural phase transitions, for understanding the properties of double perovskite oxides, is very important; and can be exemplified by the fact that, recently, a coincidence between the tetragonal to cubic phase transition temperature, the Curie temperature and the metal-insulator transition temperature has been found in Sr_2FeMoO_6 [5,6]. Although the role of the structural change is not very clear, the coincidence of the mentioned transition temperatures strongly suggests that such a relation exists.

In recent publications [7–10], we presented experimental results for the crystal structures and phase transitions of the double perovskite oxides Sr_2MWO_6 (M = Ni, Co, Mg, Zn, Cd, Ca) studied with X-ray powder diffraction method. The Co, Zn, Cd and Ca containing compounds were found to present the $P2_1/n$ (monoclinic, No. 14, non-standard setting) $\rightarrow I4/m$ (tetragonal, No. 87) $\rightarrow Fm\bar{3}m$ (cubic, No. 225) [11] phase transition sequence; for Sr_2NiWO_6, the $I4/m \rightarrow Fm\bar{3}m$ phase transition was observed; and, for Sr_2CuWO_6, experimental evidences were found that suggested the $I4/m \rightarrow I4/mmm \rightarrow Fm\bar{3}m$ phase transition sequence (later confirmed in [9] by means of neutron and synchrotron radiation diffraction measurements). In order to extend the studies of the phase transitions of the Sr_2MWO_6 compounds, we have synthesized and studied with X-ray diffraction methods the crystal structures of the title compounds. Diffraction measurements at high temperatures have been used to explore of the occurrence of structural phase transitions in these compounds.

* Corresponding author. Tel.: +34 695741545; fax: +34 946013500.
E-mail address: abdessamad.faik@ehu.es (A. Faik).

0022-2860/$ - see front matter © 2009 Elsevier B.V. All rights reserved.
doi:10.1016/j.molstruc.2009.06.008

The Sr_2MnWO_6 was originally reported as cubic, with $a = 8.01$Å [12]. More recently, the structure of the double perovskite Sr_2MnWO_6, at room temperature, was determined, by neutron powder diffraction methods, by two groups. The first study, by Azad et al. [13], described this compound as tetragonal, with the $P4_2/n$ space group (No. 86), which has never been reported for double perovskite tungstate oxides (and which is not a common tetragonal space group for double perovskite oxides), with $a = b = 8.0119(4)$Å and $c = 8.0141(8)$Å. The second work, by Muñoz et al. [14], reported the Sr_2MnWO_6 compound as monoclinic, with the $P2_1/n$ space group: $a = 5.6803(2)$Å, $b = 5.6723(2)$Å, $c = 8.0990(2)$Å and $\beta = 89.936(3)^\circ$. As it is stated in [14], in the $P4_2/n$ space group tetragonal description, it is necessary to consider three different positions for the Sr^{2+} cations and the volume of the tetragonal cell is nearly twice the monoclinic volume. Muñoz et al. [14] carried out a fitting of the crystallographic structure with the $P4_2/n$ space group: the discrepancy factors were slightly worse than those obtained for $P2_1/n$. Their conclusion was that as the structure can be described in $P2_1/n$, with a smaller unit cell and with considerably fewer atoms per unit cell and variable parameters, they preferred the monoclinic description for Sr_2MnWO_6. Moreover, they found that in the Sr_2MnWO_6 unit cell the monoclinic distortion is very small, an effect that has been widely observed in many 1:1 ordered perovskites with a strong pseudo-cubic character. Azad et al. have carried out a neutron diffraction study of Sr_2MnWO_6 at high temperatures [15], collecting data at four different temperatures, 295, 573, 773 and 973 K. In that work, they report that at 573 K, the structure remains in the same symmetry and space group, pointing out that only small changes in the refinement parameters were observed. However, at 773 K, the crystal structure changes from the primitive tetragonal symmetry (space group $P4_2/n$) to a body centered tetragonal symmetry (space group $I4/m$). And, finally, at 973 K, the crystal structure changes from body centered tetragonal symmetry to face centered cubic symmetry (space group $Fm\bar{3}m$).

The aim of the present study is twofold. First, we want to present a new route for synthesizing double perovskite oxides, which has been proven to be very efficient: low amounts of impurity are obtained, it needs lower reaction temperatures (although the grade of crystallization is good) and the samples are obtained in only two days. The second aim is to report the structural re-determination of $Sr_2Mn^{2+}WO_6$, and the structural determination of a new compound: $Sr_2Mn^{3+}WO_{6+\delta}$, by X-ray powder diffraction methods. We also present the phase transitions observed in $Sr_2Mn^{2+}WO_6$ and in $Sr_2Mn^{3+}WO_{6+\delta}$ with a survey of the evolution of the crystalline parameters according to the temperature.

2. Experimental

2.1. Sample preparation

The literature describes a large number of methods for synthesizing double perovskite oxide materials. Without any pretention of exhausting we can mention few different methods used in the last five years: ceramic method [16], sol-gel method [17], freeze-drying method [18] and exchange ionic reaction [19]. Each one has its own advantages and disadvantages. In our group, we have been using, quite successfully, the ceramic method which is well known for the easy implementation, although it can take very long synthesis time. This fact, due to the (in principle) unknown *ad hoc* thermal treatments for each compound, is usually stated as the counterpart of the easiness of the method. It has another obvious counterpart: usually, they are needed (very) high temperatures in the thermal treatment. With the aim of stablishing a good route for obtaining powder samples of double perovskite oxides, we initiated, a serial preparation of powder samples for pure and solid solution double perovskite oxides following four different methods. In this work, we report the two most efficient methods (efficiency in the sense of time and effort, in the one hand; and, in the other, in the sense of obtaining high quality samples) used for obtaining the samples of $Sr_2Mn^{2+}W^{6+}O_6$ we have analyzed.

The first one is the DTPA method, which we have used to prepare the sample 1 ($Sr_2Mn^{2+}WO_6$). As far as we know, this is the first time that the double perovskite tungstate oxide powder was prepared by the Diethylene Triamine Pentaacetic Acid (DTPA) method (sample 1). We prepared it as follows: stoichiometric amounts of $SrCO_3$, $MnCO_3$ and WO_3 were dissolved in dilute nitric solution. Then, suitable amounts of ammoniac and $C_{12}H_{20}N_3O_8$ (DTPA) (the number of moles of DTPA equals the sum of the numbers of the moles of the reagents) as coordinate agent, were added in the reactor, and a completely homogeneous light yellow transparent solution was achieved, after heating at 100 °C for 30 min, with a control of the pH between 8 and 10. This solution was subjected to evaporation, until a highly viscous residual was formed and a gel was developed during heating at 170 °C. The gel was thermally treated at 300 °C, for 5 h, and at 450 °C, for 10 h, to decompose the organic precursor. The resulting powder was heated, under nitrogen environment, progressively at different temperatures 900 °C for 10 h, 950 °C for 10 h and 1000 °C for 10 h, with intermediate regrinding. We have obtained a small amount of $SrWO_4$ as impurity (3.35%). The sample was obtained after four days, and the maximal temperature in the heat treatment was 1000 °C.

As second method of synthesis we used the co-precipitation for the preparation of sample 2 ($Sr_2Mn^{2+}WO_6$). Stoichiometric quantities of $Sr(NO_3)_2$ (I), $(OOCH_3)_2Mn \cdot 4H_2O$ (II) and $(NH_4)_{10}W_{12}O_{41}$ (III) were dissolved separately in distilled water. A slow addition, under magnetic agitation, of (III) in (I) and (II) mixture at room temperature induces the formation of a precipitation. After slow evaporation at about 60 °C, the resulting powder was heated progressively, at different temperatures, with intermediate regrinding: at 300 °C, 400 °C, 500 °C (for 8 h every temperature) and 900 °C for 24 h. The whole heat treatment was conducted under a nitrogen environment. The obtained final powder of $Sr_2Mn^{2+}WO_6$ is brown in color. In this case, we have obtained, an even lower quantity of impurity ($< 1\%$) of MnO in this sample, that was included as secondary phase in the final refinement. The sample was obtained after two days, and the maximal temperature in the heat treatment was 900 °C. Consequently, the method of co-precipitation presents the shortest time and the lowest temperature of preparation.

2.2. X-ray powder diffraction

The powder diffraction data were obtained using a Philips X'Pert MPD System with Cu K_α (Ni-filter) radiation, equipped with a proportional detector. The specimen for diffraction at room temperature was prepared by depositing sample powder on a Si plate. The intensity data were collected by continuous scanning with 2θ steps of 0.01° and counting times of 10 s at each step. The 2θ range covered was 15°–100°. X-ray diffractograms at high temperatures, $Sr_2Mn^{2+}WO_6$ and $Sr_2Mn^{3+}WO_{6+\delta}$ both in air, were obtained using an Anton Paar HTK16 temperature chamber, with a temperature stability of 0.5 K, mounted on the same diffractometer. In the case of $Sr_2Mn^{2+}WO_6$, another experiment was conducted under a vacuum environment, high temperature X-ray powder diffraction data were recorded on a Bruker D8 Advance θ/θ diffractometer, equipped with a Vantec high speed one-dimensional detector using CuK_α radiation. An Anton Paar HTK2000 high-temperature chamber with direct sample heating (Pt filament) and a temperature stability of 0.5 K was used. The data were collected using con-

tinuous scan with steps of 0.0083° (2θ) and a counting time of 1 s per step.

In both diffractometers, the specimens for the high temperature measurements were prepared by mixing the material under study with high temperature resin (Zapon lacquer). Then the mixture was 'painted' over the Pt-strip heater of the chamber. Special attention was paid to the additional peaks belonging to the Pt sample heater that are present in the high temperature diffractograms, and that overlap with the peaks originating from the samples studied. These peaks were excluded from the refinement.

The Rietveld refinement of the data was performed with WinPlotr/FullProf package [20]. The peak shape was described by a pseudo-Voigt function, and the background level was modeled using a polynomial function. The refined parameters were: scale factor, zero shift, lattice constants, peak profile, asymmetry parameters, atomic positions and independent isotropic atomic displacement parameters.The impurities were treated as known additional phases in a multiphase refinement.

2.3. Electron paramagnetic resonance

A Bruker ESP300 spectrometer operating at X band was used to record the EPR (Electron Paramagnetic Resonance) spectra of the compounds at room temperature. The magnetic field was calibrated by a NMR probe and the frequency inside the cavity was determined with a Hewlett-Packard 5352B microwave frequency counter.

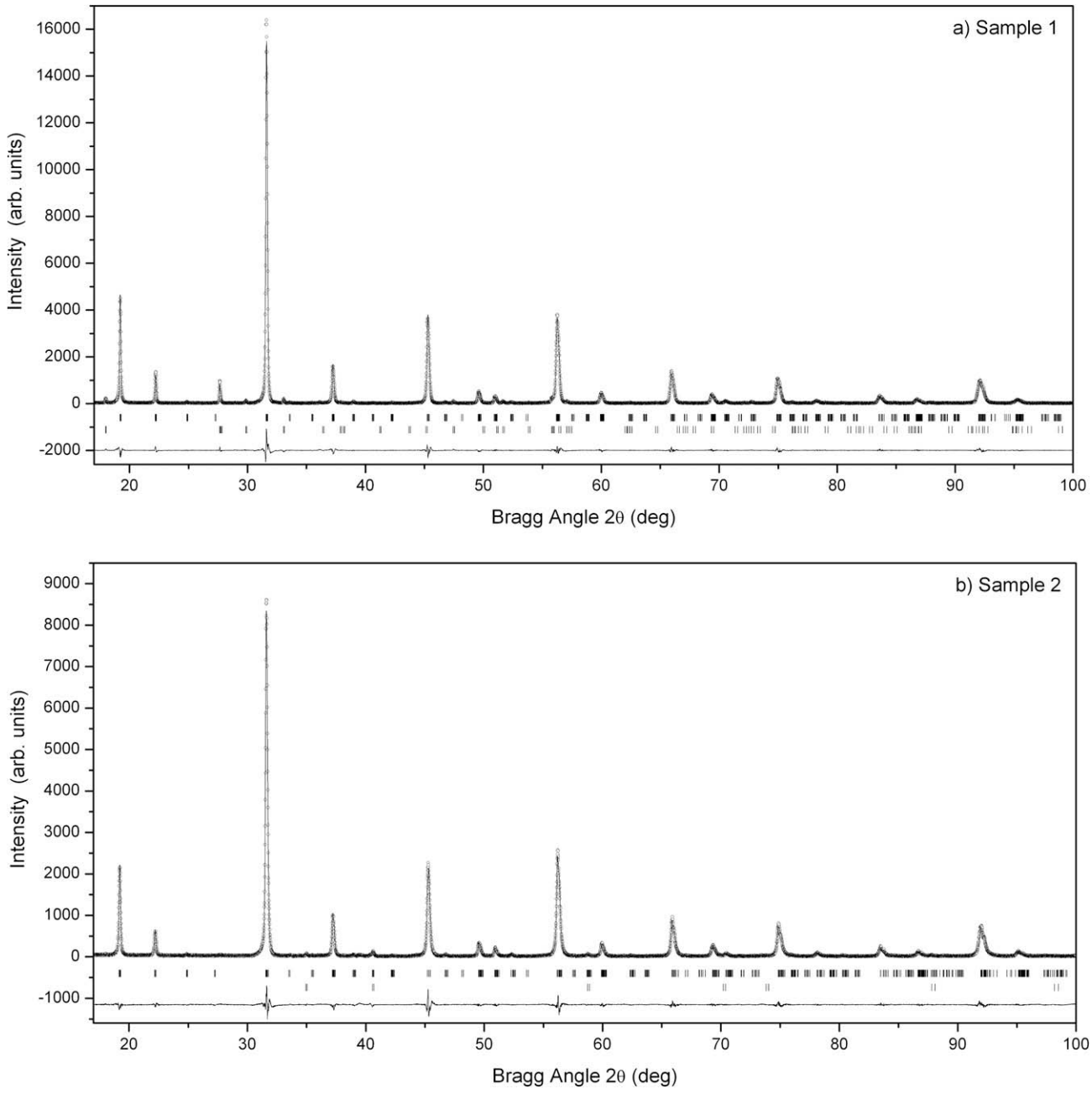

Fig. 1. Observed (·), calculated (–) and difference profiles for the Rietveld refinement of $Sr_2Mn^{2+}WO_6$ at room temperature using a structural model with the $P2_1/n$ space group. In (a), the impurity $SrWO_4$ (<3.35%) is included in the refinement as a known additional phase. In (b), the impurity MnO ($< 1\%$) is included in the refinement as a known additional phase. The top barred pattern corresponds to $Sr_2Mn^{2+}WO_6$ and the bottom barred pattern to the impurity.

2.4. X-ray absorption spectroscopy

The X-ray absorption spectroscopy (XAS) experiments in the Mn K- and the W L3-edges were carried out at the Spanish CRG beamline (SpLine-BM25). The electron beam energy of the ring was 6 GeV, and the average current was 200 mA. The energy was chosen using a Si(111) double-crystal monochromator, detuned up to a 70% of the maximum intensity to reject the components from higher harmonics. The experiments were developed in the fluorescence yield mode. Mn K and W L fluorescence lines were collected under a 90° geometry using a Si(Li) detector from e2v Scientific Instruments. The incident X-ray intensity was monitored by a gas-filled ionization chamber. Several measurements were performed on each edge to assure a good signal-to-noise ratio. The samples were mounted in a furnace and X-ray spectra were taken at several temperatures, going from room temperature to 875 K, and then again at room temperature in order to observe any variation between both room temperature spectra. The data treatment of the XANES (X-ray Absorption Near-Edge Spectroscopy) spectra were performed with the ATHENA software [21].

2.5. Neutron powder diffraction

The neutron diffraction measurements were performed in the D20 high-intensity, medium-resolution instrument at Institut Laue-Langevin (ILL, Grenoble, France). The diffraction profiles were collected in the range $2\theta = 0 - 160°$ with a neutron wavelength of 1.3 Å. The monochromator was Cu(200). This instrument is equipped with a detector that covers 153.4° in 2θ space and is made of 1534 ^{3}He cells [22]. The samples were placed in a vanadium capillary of 5 mm in diameter. Continuous heating with a rate of 1 K/min from room temperature to 1200 K were performed using a vanadium furnace in order to monitor the temperature-induced structural transitions. The coherent scattering lengths for Sr, Mn, W and O were 8.24, −3.75, 4.77 and 5.805 fm, respectively.

3. Results and discussion

3.1. Room-temperature structures

In Fig. 1 we show the X-ray diffraction results, at room temperature, for samples 1 and 2. As mentioned, $P4_2/n$ [13] and $P2_1/n$ [14] space groups have been proposed, using neutron powder diffraction data, for the room-temperature structure of Sr_2MnWO_6. We tried both structures as the starting models for our refinements; the *R*-factor values obtained (sample 2) for both space groups are: $R_p = 10.6\%; R_{wp} = 16.0\%; R_{exp} = 10.11\%; \chi^2 = 2.50$ for $P4_2/n$ with 8 atoms per unit cell; and $R_p = 7.96\%; R_{wp} = 12.5\%; R_{exp} = 8.77\%; \chi^2 = 2.02$ for $P2_1/n$ with 6 atoms per unit cell; as we can see, the best *R*-factor values were obtained for the monoclinic model with fewer atoms per unit cell and smaller primitive unit cell volume ($V_T \simeq 2V_M$). Thus, we suggest that the room-temperature space group of $Sr_2Mn^{2+}WO_6$ is $P2_1/n$. There are three facts that support this affirmation. First, it is very easy to confirm that the $P4_2/n$ space group is not common; indeed it is very strange, as a space group preferred by double perovskites (although it is a possible one). Secondly, there is a "crystallographic reason" also used by Muñoz [14]: there is a little improvement in the *R* factors when the structure is described using the $P4_2/n$ space group, which needs a bigger unit cell (primitive) and which gives rise to more degrees of freedom, as, for instance, instead of having only one Sr cation position, there are three. Thirdly, in a previous paper [10], we presented a phase diagram (transition temperature vs. tolerance factor) in the Sr_2MWO_6 family. The data in that figure demonstrate that the Sr_2MWO_6 family (including a continuous solid solution $Sr_2Cd_{1-x}Ca_xO_6$ [23]) shows the same phase-transition sequence $P2_1/n - I4/m - Fm\bar{3}m$, and the feature of increasing the stable temperature range of the more distorted monoclinic phase and the diminishing of the tetragonal $I4/m$ phase as the tolerance factor diminishes at room temperature. We see no "physical" reason to take out the present work compound from that general behaviour (trend) proven to exist in the mentioned family. With all these arguments, we conclude that the correct space group assignation for the room-temperature structure of Sr_2MnWO_6 is undoubtedly the monoclinic $P2_1/n$. The results obtained for the crystal structure of $Sr_2Mn^{2+}WO_6$ at room temperature and the reliability parameters of the refinement are given in Table 1. Similar results were obtained using samples 1 and 2 data.

Table 1
Crystal structure data and refinement results for $Sr_2Mn^{2+}WO_6$ at room temperature. The atomic positions (in fractional coordinates) and temperature factors were refined in the space group $P2_1/n$. (Note: $a = 5.6764(1)$Å; $b = 5.6752(1)$Å; $c = 8.0144(1)$Å; $\beta = 90.12(1)°$ and $V = 258.18(1)$Å^3; $R_p = 7.96\%; R_{wp} = 12.5\%; R_{exp} = 8.77\%; \chi^2 = 2.02$).

Atom	Site	*x*	*y*	*z*	B(Å^2)
W	2a	0	0	0	0.27(3)
Mn	2b	1/2	1/2	0	0.10(1)
Sr	4e	0.0054(7)	0.5166(3)	0.2464(7)	0.67(4)
O1	4e	0.057(2)	0.020(2)	-0.236(1)	0.92(8)
O2	4e	0.252(1)	-0.221(5)	0.042(4)	0.92(8)
O3	4e	0.210(5)	0.264(5)	0.038(2)	0.92(8)

In Fig. 2 we show the X-ray diffraction measurement results obtained using sample 2 at different temperatures between 470 and 1090 K, in three selected 2θ ranges: (44.0°–46.0°), (55.0°–57.0°) and (73.5°–76.0°). The main goal of this experiment was to determine precisely the temperature of the known to exist two phase transitions [15]: in that work, the authors reported three different structures: $P4_2/n$, at room-temperature; $I4/m$, at 573 K and $Fm\bar{3}m$, at 773 K. At a first glance to Fig. 2, it seemed that our results could be compatible with the known two phase-transition sequence in Sr_2MnWO_6. We thought that the phase-transitions temperatures were approximately 630 and 820 K, as indicated by the white dot-lines in Fig. 2. Nevertheless, the behavior between 820 and 1020 K temperatures puzzled us: in that temperature interval, the cell parameters of the compound diminished. We interpreted it as a possible irreversible transformation, taking place continuously in temperature, to another compound; in fact, the color of the recovered sample had changed from brownish to black; and, besides, a great increase in the amount of impurity present in the sample was noticed.

In Fig. 3 we show the results obtained in the 2θ angular range (15°–100°) for sample 2: (a) before increasing the temperature from room temperature to 875 K and (b) after recovering the room-temperature conditions. The amount of impurity has noticeably increased; and, what is more important, the starting phase is not recovered; hence, the compound has, undoubtedly, transformed irreversibly (see below, next sub-section $Sr_2Mn^{3+}WO_{6+\delta}$). Having this fact in mind, we re-interpreted the results shown in Fig. 2: up to approximately 820 K, the compound keeps the structure of $Sr_2Mn^{2+}WO_6$, and at that temperature, it starts to transform irreversibly. Thus, the temperature interval of interest to observe the previously reported phase transitions is 473–773 K; although in our results, in that temperature interval only one clear anomaly was seen.

The behavior of the three sets of reflections, shown in Fig. 2, is qualitatively the same. At ≈ 810 K, the evolution with temperature

of all them changes and instead of evolving to lower 2θ values, they move to higher values. This is a sign of a decreasing of the cell parameters. As a possible explanation to this observation, we thought that the $Sr_2Mn^{2+}W^{6+}O_6$ compound transformed to $Sr_2Mn^{3+}W^{5+}O_6$; thus, we thought of an oxidation–reduction transformation. There are some facts supporting that conclusion. First, the conventional X-ray measurements have been done in air, and it is known how easily Mn^{2+} oxides in air. Second, we can compare the ionic radii of Mn^{3+} (0.645 Å) and W^{5+} (0.620 Å) to those of Mn^{2+} (0.830 Å) and W^{6+}(0.600 Å). Although the ionic radius reduction in the tungstate is very small ($\Delta r_W = 0.02$ Å), in the manganese after the proposed transformation the reduction is one order of magnitude bigger ($\Delta r_{Mn} = 0.195$Å), and, relatively, it is a 30% decrease. So, it is quite reasonable to think of a general unit cell reduction, as the inter-atomic distances are governed by the ionic radii. This reduction, in turn, will appear as an evolution with temperature of the position of the reflections to bigger values of 2θ, at least, while the oxidation–reduction transformation takes place. Once it has finished, it is supposed that the cell parameters will be evolve with temperature as usual.

We made a thermal treatment in $Sr_2Mn^{2+}W^{6+}O_6$: we heated it in air at 875 K, during 24 h. The sample was heated up and cooled down slowly 3 K/min. After the treatment, we obtained the same two features in the recovered sample (sample 3): color had changed to black, and a big amount of impurity was present.

To confirm our assumption about the mechanism of the observed transformation, we recorded an EPR spectrum, at room temperature, for both samples: $Sr_2Mn^{2+}W^{6+}O_6$ (sample 2) and sample 3. Fig. 4 shows the EPR spectra obtained. The EPR signal shows a broad isotropic signal centred at a resonance field of 3367.4(2) Oe, corresponding to g value of 1.998(1), indicating that manganese ions are in the 2+ oxidation state in sample 2; besides,

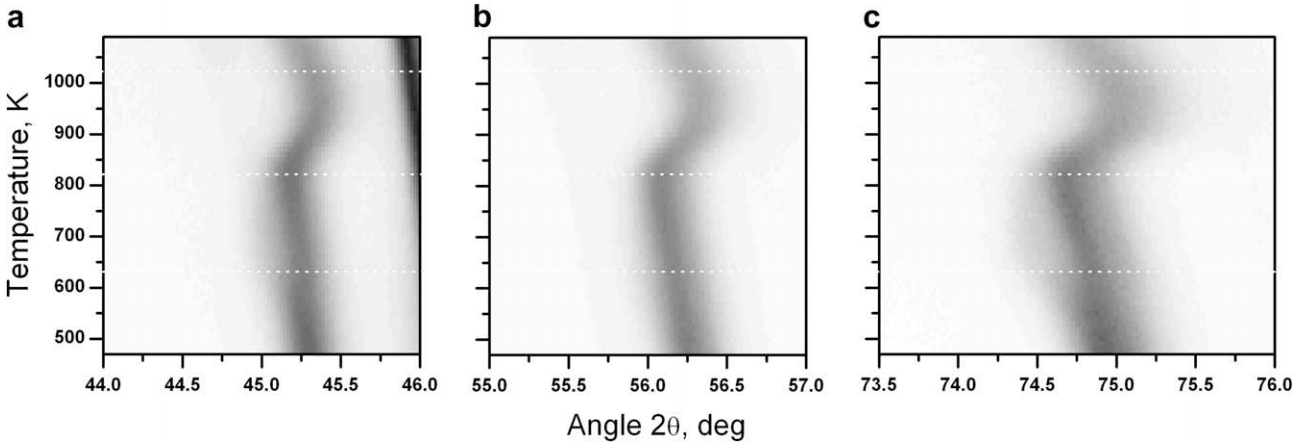

Fig. 2. Temperature evolution of the three diffraction line-set at $2\theta \approx 45^\circ; 56^\circ; 75^\circ$, obtained by X-ray diffraction measurement in air of $Sr_2Mn^{2+}WO_6$ (sample 2). At 640 K, the compound transforms to the tetragonal $I4/m$ space group. Before the expected high-temperature cubic ($Fm\bar{3}m$ space group) phase appears, the $Sr_2Mn^{2+}WO_6$ compound starts to transform irreversibly to $Sr_2Mn^{3+}WO_{6+\delta}$, at about 820 K.

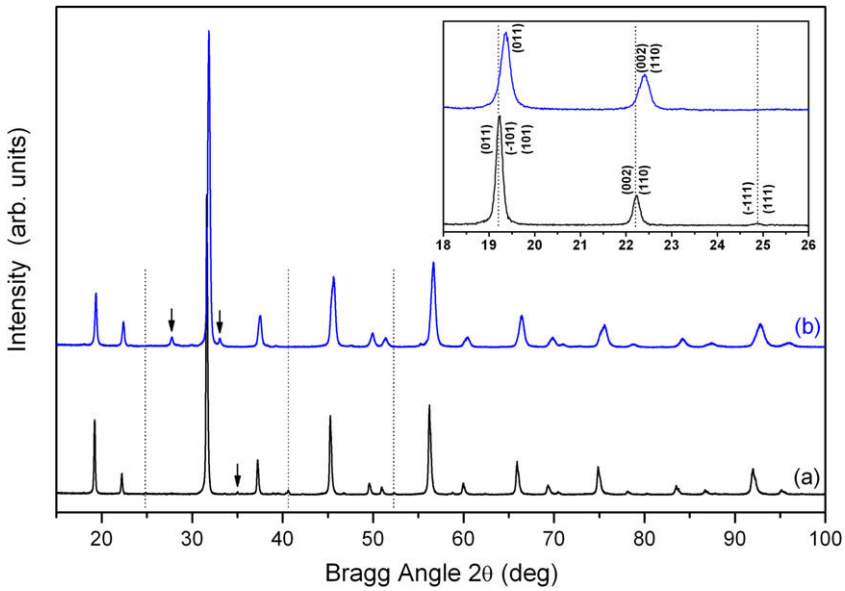

Fig. 3. X-ray diffraction patterns of (a) $Sr_2Mn^{2+}WO_6$ (sample 2) and (b) $Sr_2Mn^{3+}WO_{6+\delta}$ (sample 3). In the inset we have enlarged the 2θ-interval, and we have indicated the indices of the reflections in the $P2_1/n$ and $I4/m$ space groups, for (a) and (b), respectively. The (111/111) reflections characteristic of a primitive cell are clearly seen in (a). Another two peaks which are absent are highlighted by dashed vertical lines. The arrows at 27.7°, 32.9° and 34.9° show the Peaks due to the impurities of $SrWO_4$, $Sr_2Mn_2O_5$ and MnO, respectively.

there is no signal at all in the case of sample 3, indicating that there is no manganese cations in it in the 2+ oxidation state, and, thus, that all the manganese present is in 3+ oxidation state.

As we performed the thermal treatment on $Sr_2Mn^{2+}W^{6+}O_6$ in air, it could had happened that while Mn^{2+} oxided to Mn^{3+}, the sample had gained some oxygen, maintaining the W^{6+} oxidation state; thus, transforming to $Sr_2Mn^{3+}W^{6+}O_{6+\delta}$; or, otherwise, to maintain charge neutrality, the W^{6+} cation could had transformed to W^{5+}, therefore, the compound in sample 3 should be $Sr_2Mn^{3+}W^{5+}O_6$. In order to see if the sample gains oxygen or W^{6+} transforms to W^{5+}, while the temperature is increased in air, we focused on the oxidation states of manganese and tungsten at room temperature, after and before the thermal treatment at 875 K.

The XANES experiments at the Mn K-edge and W L3-edge were carried out for the starting material $Sr_2Mn^{2+}W^{6+}O_6$ and the treated sample, and normalized spectra are shown in Fig. 5. The Mn K-edge XANES spectra recorded at room temperature on sample 2, as prepared and after the thermal treatment at 875 K are depicted in Fig. 5(a). As it is clear form the figure, changes in the absorption edge occurred after the thermal treatment: the edge position shifts from 6543 to 6550 eV, revealing the transition from Mn^{2+} to Mn^{3+}. Furthermore, the spectrum profile of the starting Mn^{2+} double perovskite resembles to analogue perovskites with Fe^{2+}, whereas the shape of the Mn^{3+} treated sample is very similar to Fe^{3+} perovskites [24,25]. The W L3-edge XANES spectra recorded at room temperature, before and after thermal treatment are extremely similar to each other, as shown in Fig. 5(b). The position of the

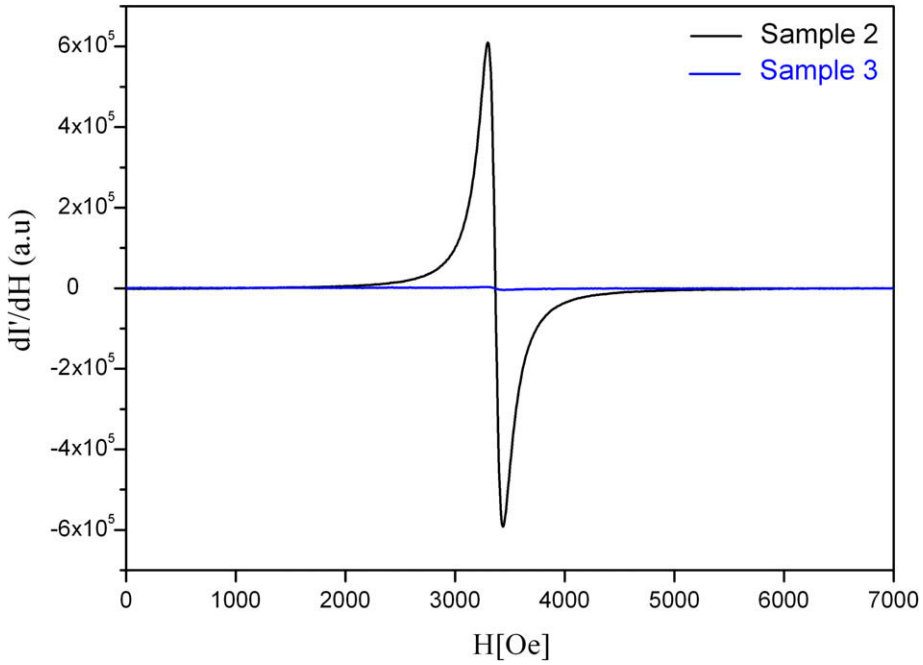

Fig. 4. Room-temperature EPR spectrum of samples 2 and 3. The EPR signal shows a broad isotropic signal, centred at a resonance field of 3367.4(2) Oe, corresponding to *g* value of 1.998(1), indicating that manganese ions are in the 2+ oxidation state in sample 2; besides, there is not signal at all in the case of sample 3, indicating that there is no manganese cations in it in the 2+ oxidation states, and, thus all the manganese present is in 3+ oxidation state.

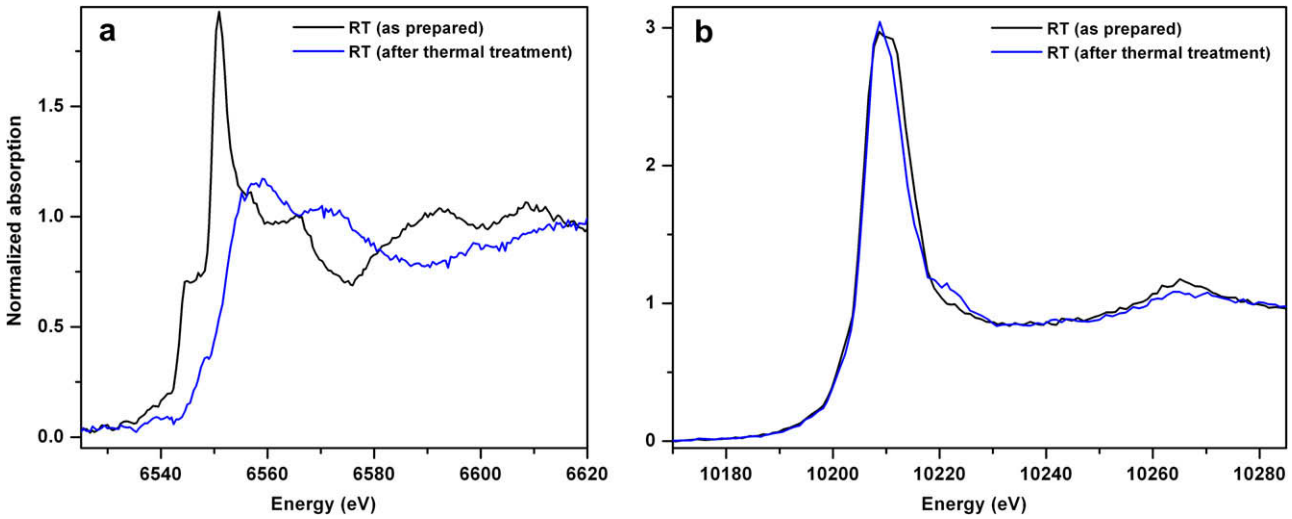

Fig. 5. XANES spectra, at room temperature, of sample 2 (as prepared) and sample 3 (after the thermal treatment at 875 K): (a) Mn K-edge, (b) W L3-edge.

W edge absorption at the half jump in the as-prepared sample is found at 10205 eV, a typical value for tungsten in the 6+ oxidation state [25,26]. The treated sample has the same edge energy, the W L3 edge usually does not present an important shift in the edge energy, in this case the edge position is the same, suggesting the maintenance of a W^{6+} oxidation state [25]. The L3 absorption edge comes from a direct dipolar $2p \rightarrow 5d$ transition, so the slight differences in the double structure in the white line may suggest a weakening of the crystal field effect in the WO_6 octahedra, due to increase in the W–O distances in the transition to the tetragonal symmetry. Thus, from the combined EPR and XANES measurements results, we conclude that $Sr_2Mn^{2+}W^{6+}O_6$ transforms, at 875 K in air, to $Sr_2Mn^{3+}W^{6+}O_{6+\delta}$. Of course, the non-stoichiometric excess in oxygen compensates the change in the oxidation state in Mn and the maintenance of the oxidation state in W. This transformation is irreversible, and, thus, in turn, gives rise to a new material.

We focused in this new material and we made a room-temperature X-ray diffraction measurement in $Sr_2Mn^{3+}WO_{6+\delta}$ (sample 3). In addition to the already mentioned color change and impurity increase, the diffractogram has two more features: (i) it is relatively shifted to higher angles (Fig. 3, in comparison to the results obtained before the thermal treatment, sample 2), what is consistent with a decrease in the cell parameters; and (ii) there are some reflections pertaining to the monoclinic phase that have disappeared (marked with dashed lines); a fact that can be interpreted as a symmetry increase. The reflections that disappear are of the type (hkl) with $h+k+l=2n+1$, which are characteristic of a primitive cell. Bearing in mind that the are characteristic of a primitive cell, we performed a refinement with a tetragonal space group, $I4/m$, and using the structural results obtained for sample 2 with the tetragonal phase as the starting structural model. The results of the refinement are shown in Fig. 6, and the final structural results and refinement parameters obtained are summarized in Table 2. The results of refinements shown the presence of 2.90% of $SrWO_4$ and 1.37% of $Sr_2Mn_2O_5$, which mean a partial decomposition of the compound to 2:1 mole proportional portion of $SrWO_4$ and $Sr_2Mn_2O_5$, respectively, according to the following chemical reaction: $Sr_2MnWO_6 + 1/2O_2 \rightarrow 2SrWO_4 + Sr_2Mn_2O_5$. We conclude that the sample 3 allows for 2:1:1 proportional portion of Sr, Mn and W, respectively.

Table 2
Crystal structure data and refinement results for $Sr_2Mn^{3+}WO_{6+\delta}$ at room temperature. The atomic positions (in fractional coordinates) and temperature factors were refined in the space group $I4/m$. (Note: $a = 5.6353(1)$ Å; $c = 8.0149(1)$ Å and $V = 254.53(1)$Å^3; $R_p = 10.6\%$; $R_{wp} = 15.1\%$; $R_{exp} = 5.42\%$; $\chi^2 = 7.73$).

Atom	Site	x	y	z	B(Å^2)
W	2a	0	0	0	0.33(7)
Mn	2b	0	0	1/2	0.37(2)
Sr	4d	0	1/2	1/4	0.74(3)
O1	4e	0	0	0.241(2)	1.05(4)
O2	8h	0.219(2)	0.276(1)	0	1.05(4)

Unfortunately, the refinement of oxygen site occupancy was not very conclusive, due to the insensitivity of powder X-ray diffraction to small variations in oxygen content in the presence of higher atomic number elements. Nevertheless, the refinement results are consistent with fixed occupancy of these sites. The oxygen occupancy at the 4*e* and 8*h* sites ($I4/m$ space group) was fixed during the refinement at 1 and 1.125, respectively, as the initial stoichiometry seemed most likely to be $Sr_2Mn^{3+}WO_{6.5}$. The mean interatomic distances of Mn and W in $Sr_2Mn^{2+}WO_6$ and $Sr_2Mn^{3+}WO_{6+\delta}$ are listed in Table 3. In the case of $Sr_2Mn^{2+}WO_6$, the bond lengths of $Mn-O1, Mn-O2$ and $Mn-O3$ are 2.139(3), 2.145(8) and 2.144(8) Å, respectively, which are very close and similar to the value predicted by bond valence calculations 2.196 Å. The same results are observed for the bond lengths of WO_6 octahedra. In the other compound $Sr_2Mn^{3+}WO_{6+\delta}$, the bond lengths in the axial position of Mn are elongated due to a Jahn-Taller distortion. In consequence, we have obtained two large distances 2.076(1) Å and four short distances 2.024(7) Å, the average value of the Mn bond distances within the octahedra 2.041(2) Å are in good agreement with the value predicted by bond valence calculations 2.0461 Å. As sequences we have obtained deformed WO_6 octahedra, with two short axial distances 1.930(1) Å and four large distances 1.986(7) Å.

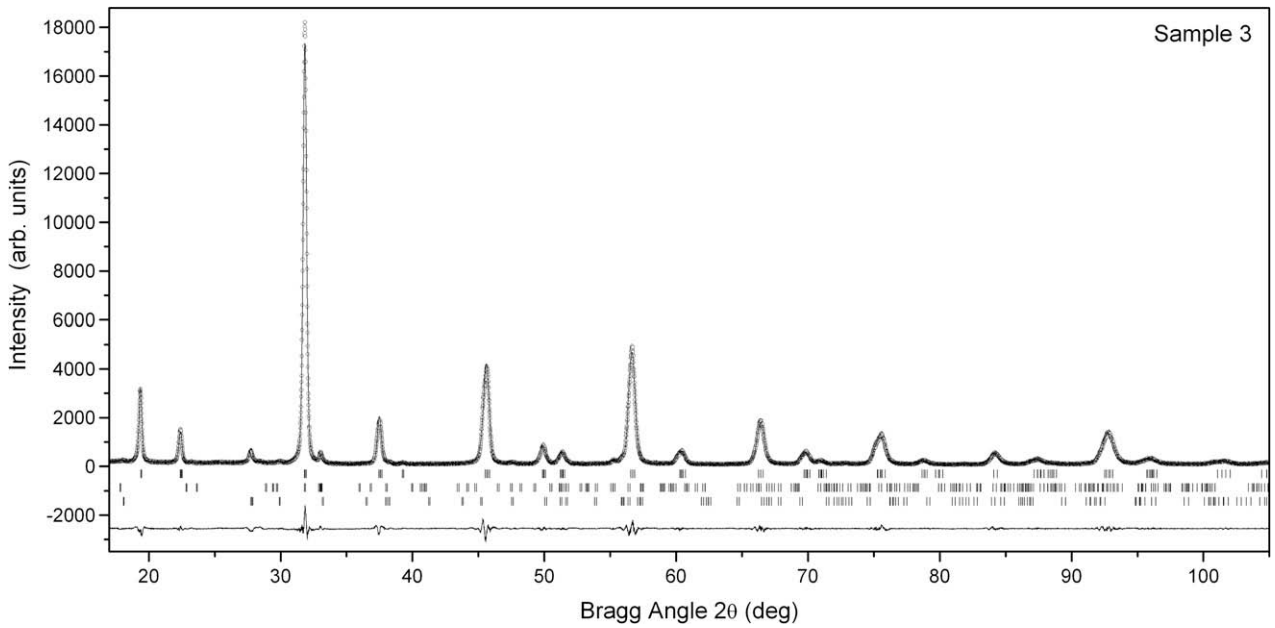

Fig. 6. Observed (·), calculated (–) and difference profiles for the Rietveld refinement of $Sr_2Mn^{3+}WO_{6+\delta}$ (sample 3) at room temperature using a structural model with the $I4/m$ space group. The top barred pattern corresponds to $Sr_2Mn^{3+}WO_{6+\delta}$, and the middle and bottom barred patterns to the impurities $SrWO_4$ (2.90) and $Sr_2Mn_2O_5$ (1.37), respectively, which have been included in the refinement as known additional phases.

Table 3
Main bond distances (Å) for $Sr_2Mn^{2+}WO_6$ and $Sr_2Mn^{3+}WO_{6+\delta}$ from XRPD at room temperature.

	$Sr_2Mn^{2+}WO_6$	$Sr_2Mn^{3+}WO_{6+\delta}$
Mn-O1	2.139(3) (×2)	2.076(1) (×2)
Mn-O2	2.145(8) (×2)	2.024(7) (×4)
Mn-O3	2.144(8) (×2)	–
Average distance	2.143(9)	2.041(2)
Predicted distance	2.196	2.046
W-O1	1.926(3) (×2)	1.930(1) (×2)
W-O2	1.931(8) (×2)	1.986(7) (×4)
W-O3	1.938(8) (×2)	–
Average distance	1.932(9)	1.967(2)
Predicted distance	1.917	1.946

3.2. High-temperature phase transitions in $Sr_2Mn^{2+}WO_6$

To determine precisely the temperatures of the expected phase transitions in $Sr_2Mn^{2+}WO_6$ (sample 2), we performed neutron and X-ray powder diffraction (XRPD) measurements at different temperatures, under vacuum (to avoid the sample transformation to $Sr_2Mn^{3+}WO_{6+\delta}$). In Fig. 7(a) and (b) we show the results obtained from neutron measurements, in the 430–750 K temperature interval, with a 1 K step, in the (44.0°–41.5°) and (49.0°–50.75°) selected 2θ intervals, corresponding to the primitive Bragg peaks $(131/\bar{1}31/311/\bar{3}11)$ and $(124/\bar{1}24/214/230/\bar{2}14/320)$, respectively. It can be seen clearly that these peaks, of the type *hkl* which not satisfy the $h + k + l = 2n$ reflection condition, gradually disappear at about 640 K. This observation indicates that at about 640 K, the structure transforms from primitive unit cell to a centered unit cell. Unfortunately the neutron diffraction measurement could not show significant changes for the rest of the peaks in the temperature range 430–1200 K. This is because D20 is a resolution limited instrument. The disappearance of the primitive Bragg peaks is also observed in the X-ray diffraction measurement results. For example, in Fig. 7(c), the peaks $(124/\bar{1}24/214/230/\bar{2}14/320)$, observed in (58.0°–59.5°) 2θ interval, disappear at the same temperature 640 K. Fig. 8 shows the results obtained by X-ray diffraction mea-

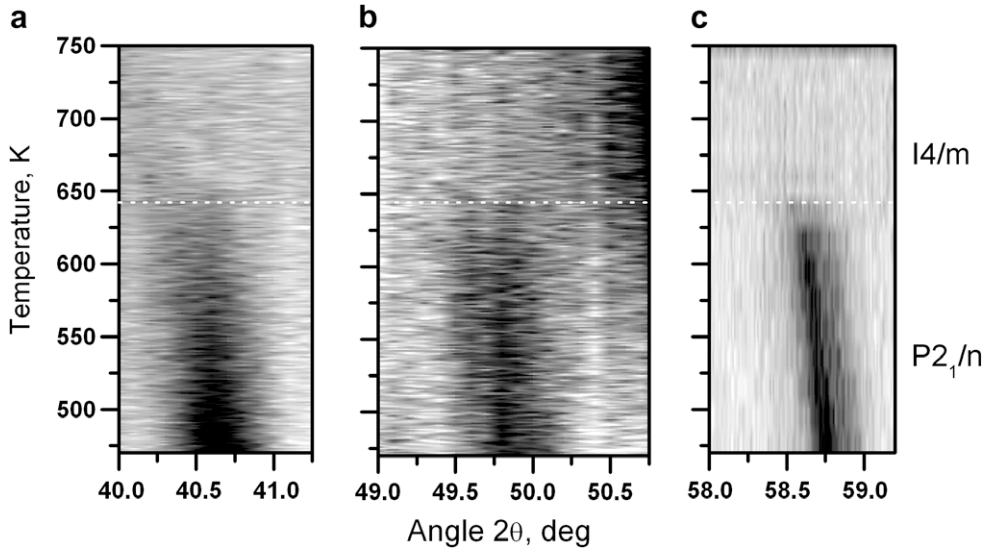

Fig. 7. Thermal evolution of the primitive Bragg peaks of $Sr_2Mn^{2+}WO_6$ obtained under vacuum from neutron powder diffraction (a and b) and from XRPD experiments (c). The scattered intensity is represented with gray scale, black being high intensity and white lowest intensity. Thermal evolution of $(131/\bar{1}31/311/\bar{3}11)$ in (a) and $(124/\bar{1}24/214/230/\bar{2}14/320)$ in (b and c), showing the disappearance of these peaks at about 640 K.

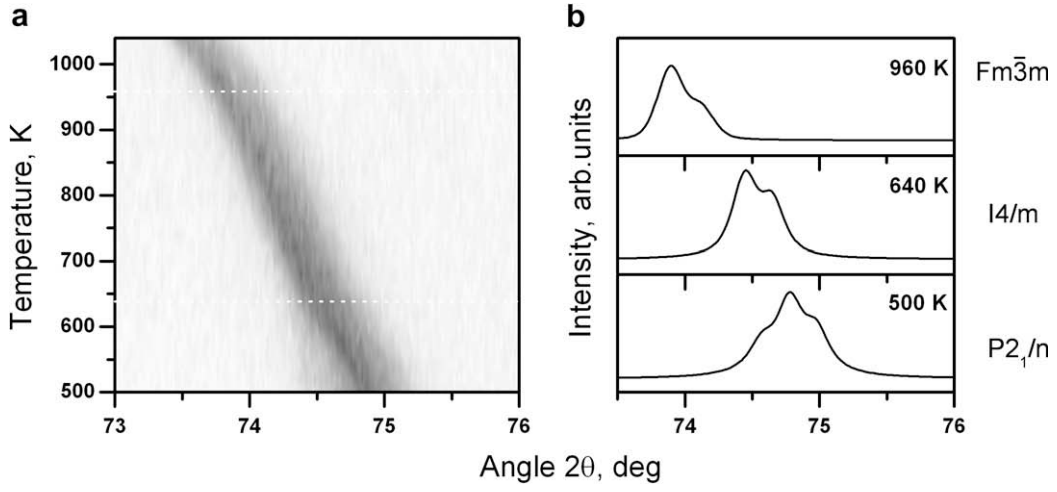

Fig. 8. Thermal evolution of (620) cubic reflections as obtained from XRPD experiments under vacuum of $Sr_2Mn^{2+}WO_6$. The scattered intensity is represented with gray scale, black being high intensity and white lowest intensity. The monoclinic triplet converts to a tetragonal doublet reflection at the same temperature of disappearance of the primitive Bragg peaks, and, eventually, the tetragonal splitting disappearance and the double reflection evolves to a single cubic one at about 960 K.

surements in the (73°–76°) 2θ selected interval, corresponding to (620) cubic reflection. At all temperatures covered, the 2θ region chosen for the phase transition search contains a group of diffraction peaks that has been identified as especially sensitive to the structural changes occurring in double perovskite materials [8]. The monoclinic triplet converts to a tetragonal doublet reflection at the same temperature at which the primitive Bragg peaks disappear, and, eventually, the tetragonal splitting disappears and the double reflection evolves to a single cubic one at about 960 K. This behavior is very similar to that observed, for instance, in Sr_2CaWO_6 [8], where these changes were interpreted as evidence of the material undergoing two phase transitions: first, from a monoclinic structure to a tetragonal one, and (at higher temperature) then from tetragonal to cubic.

Next, we measured sample 2 in the (17°–80°) 2θ range and in the temperature interval from 500 to 1040 K, with a temperature step of 20 K, to have good enough data to determine the variation of the cell parameters with temperature. In Fig. 9 we show the results obtained for the variation with temperature of the cell parameters (a) and unit cell volume (b), in sample 2. Up to 640 K the compound is monoclinic ($P2_1/n$); from 640 to 940 K it is tetragonal ($I4/m$); and it remains cubic ($Fm\bar{3}m$), from 960 up to 1040 K. It can be observed that, in the monoclinic phase, the metric parameters ($b\sqrt{2}$, c) change continuously, and, at 640 K, become almost equal. The observed phase-transition sequence, $P2_1/n \rightarrow I4/m \rightarrow Fm\bar{3}m$, is the "usual" two phase-transition sequence encountered in some of the members of the double perovskite tungstate oxide family, and connects the three space groups most frequently found for the ordered perovskites.

3.3. High-temperature phase transitions in $Sr_2Mn^{3+}WO_{6+\delta}$

As in the previous case, the search for phase transitions was carried out by performing diffraction measurements of sample 3, in the (17°–80°) 2θ range and in the temperature interval from 320 to 870 K, with a temperature step of 20 K, to have good enough data to determine the variation of the cell parameters with temperature. The temperature dependence of the cell parameters (a) and unit cell volume (b), is shown in Fig. 9. At about 710 K a strong discontinuous phase transition is observed. The high temperature phase is indexed as cubic $Fm\bar{3}m$ and the low temperature one as tetragonal, body centered. No changes in the set of observed reflections were found below this temperature, suggesting that the unit cell does not change in the temperature range from 700 K to room temperature. However, at about 490 K a very small change in the slope of the curve of variation of the c tetragonal cell parameter is observed (in Fig. 9 we have shown the prolongation of the temperature evolution of the $I4/mc$ cell parameter with a dashed line as guide for the eyes). This behavior is compatible with a continuous phase transition.

In a double perovskite structure with the $I4/mmm$ space group the octahedra are not rotated, therefore, there is no change in the intensity of some reflections with temperature. In a double perovskite structure with the $I4/m$ space group, however, the octahedra are rotated. In this case, there is a change in the intensity of some reflections with the rotation angle: the bigger the value of the rotation angle, the smaller the height of the peaks. Thus, the assumption that there is a continuous phase transition at 490 K, for which the order parameter is proportional to the rotation angle, could explain the change of the cell parameters observed in Fig. 9. The XRPD are not suitable for these observations, and the NPD data that we have are not good enough for seeing these intensity changes. But, if we assume that at 490 K there is a phase transition under way, this (very small) anomaly could be explained as produced by the homogeneous strain coupled to the order parameter. It is not easy to observe a transition of the type $I4/m \rightarrow I4/mmm$, because the two space groups have the same extinction conditions (no peak splitting or appearance of new

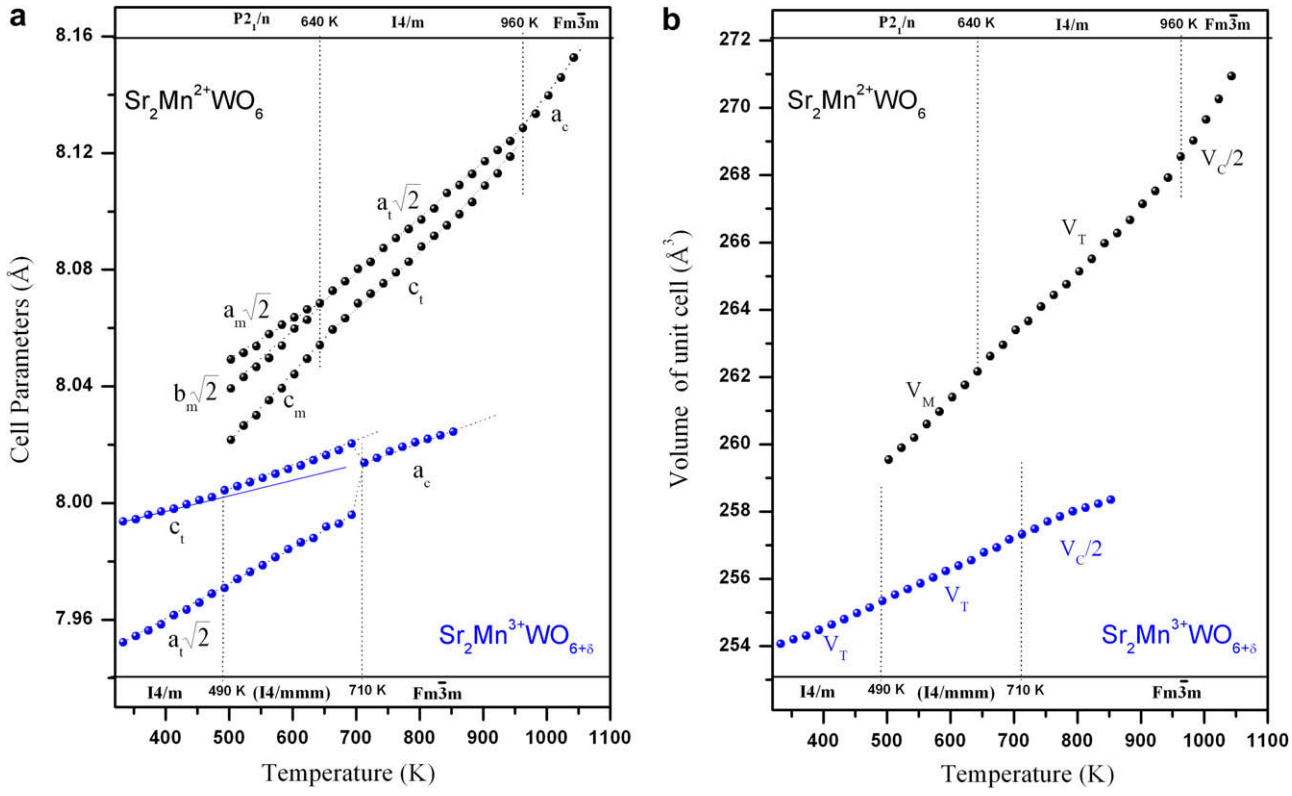

Fig. 9. Variation with the temperature of the cell parameters (a) and unit cell volume (b) of $Sr_2Mn^{2+}WO_6$ and $Sr_2Mn^{3+}WO_{6+\delta}$, as indicated.

peaks is expected). It should also be pointed out that the refinement of the room temperature structure in the $I4/m$ space group gives better reliability parameters than the refinement in the $I4/mmm$ group, although the difference is small. This is due to the fact that X-ray diffraction is not very sensitive to the positions of the oxygen atoms. The fact that the transition is continuous makes most of the thermal analysis methods unsuitable for its detection. The evidence presented here is not enough to affirm the existence of such a transition. However, in the analysis that we made in $Sr_2Cu^{2+}WO_6$ double perovskite [9], we showed that due to the Jahn-Teller character of the Cu^{2+} cation there was an intermediate phase between the low-temperature $I4/m$ and the High-temperature $Fm\bar{3}m$ phase, $I4/mmm$: we suggested that the lowering of the symmetry from $Fm\bar{3}m$ to $I4/m$ in $Sr_2Cu^{2+}WO_6$ was performed in two steps, $Fm\bar{3}m \rightarrow I4/mmm \rightarrow I4/m$. Now, we suggest that, being Mn^{3+} Jahn-Teller active, the same behavior could be expected for $Sr_2Mn^{3+}WO_{6+\delta}$.

The variations of the lattice parameters $a\sqrt{2}$, c and V with temperature in $Sr_2Mn^{3+}WO_{6+\delta}$ are presented in Fig. 9, all of them increase monotonously with increasing temperature. They are smaller than those observed for $Sr_2Mn^{2+}WO_6$, due to the difference between the ionic radii of Mn^{3+} (0.645 Å) and Mn^{2+} (0.830 Å).

4. Conclusions

We present, the new effective route for synthesizing Sr_2MWO_6 double perovskite oxides as the co-precipitation method because it needs a lower maximum temperature of thermal treatment and only two days of preparation. Moreover, the samples obtained in this way contain a very low quantity of impurity. Using conventional X-ray diffraction methods, we have confirmed the room-temperature space group of $Sr_2Mn^{2+}WO_6$ to be $P2_1/n$, and we have shown that the compound presents the following temperature induced phase-transition sequence: $P2_1/n \rightarrow I4/m \rightarrow Fm\bar{3}m$. After a thermal treatment, 24 h at 870 K in air, the $Sr_2Mn^{2+}WO_6$ compound transforms irreversibly to $Sr_2Mn^{3+}WO_{6+\delta}$. This transformation has been confirmed by EPR and XANES measurements. Also, we have confirmed the room-temperature space group of $Sr_2Mn^{3+}WO_{6+\delta}$ to be $I4/m$, and we have shown that the compound presents the following temperature induced phase-transition sequence: $I4/m(\rightarrow I4/mmm) \rightarrow Fm\bar{3}m$. The tetragonal-to-tetragonal phase transition is suggested to be present (taking into account the behavior of Sr_2CuWO_6), not seen as it is very weak; and it is attributed to the presence of the Jahn-Teller active Mn^{3+} cation.

Acknowledgments

This work was done in part under Project Nos.: UPV 0063.310-13564/2001-2007 and MAT2008-05839/MAT. The authors thank the Spanish Ministry of Science for the beamtime allocation and the staff of Spanish CRG beamline (SpLine-BM25) of ESRF for their support during the experiment. We also thank ILL for the beamtime allocation and the staff of D20 for their kind help and technical assistance.

References

[1] K.-I. Kobayashi, T. Kimura, H. Sawada, K. Terakura, Y. Tokura, Nature 395 (1998) 677–680.
[2] M. DeMarco, H.A. Blackstead, J.D. Dow, M.K. Wu, D.Y. Chen, E.Z. Chien, H. Haka, S. Toorongian, J. Fridmann, Phys. Rev. B 62 (2000) 14301–14303.
[3] Y. Todate, J. Phys. Chem. Solids B 60 (1999) 1173.
[4] Y. Tomioka, T. Okuda, Y. Okimoto, R. Kumai, K.-I. Kobayashi, Phys. Rev. B 61 (2000) 422.
[5] O. Chmaissem, R. Kruk, B. Dabrowski, D.E. Brown, X. Xiong, S. Kolesnik, J.D. Jorgensen, C.W. Kimball, Phys. Rev. B 62 (2000) 14197.
[6] Y. Moritomo, Sh. Xu, A. Machida, T. Akimoto, E. Nishibori, M. Takata, M. Sakata, K. Ohoyama, J. Phys. Soc. Japan 69 (2000) 1723.
[7] M. Gateshki, J.M. Igartua, E. Hernández-Bocanegra, J. Phys.: Cond. Matter 15 (2003) 6199–6217.
[8] M. Gateshki, J.M. Igartua, J. Phys.: Cond. Matter 16 (2004) 6639–6649.
[9] M. Gateshki, J.M. Igartua, J. Phys.: Cond. Matter 15 (2003) 6749–6757.
[10] M. Gateshki, J.M. Igartua, A. Faik, J. Sol. State Chem. 180 (2007) 2248–2255.
[11] T. Hahn (Ed.), International Tables for Crystallography, vol. A, Kluwer, Dordrecht, 2002.
[12] L.H. Brixner, J. Phys. Chem. 64 (1960) 165.
[13] A.K. Azad, S. Ivanov, S.G. Eriksson, H. Rundlöf, J. Eriksen, R. Mathieu, P. Svedlindh, J. Magn. Magn. Mater. 237 (2001) 124–134.
[14] A. Muñoz, J.A. Alonso, M.T. Casais, M.J. Martínez-López, M.T. Fernádez-Díaz, J. Phys.: Cond. Matter 14 (2002) 8817–8830.
[15] A.K. Azad, S.G. Eriksson, Solid State Commun. 126 (2003) 503–508.
[16] A. Faik, M. Gateshki, J.M. Igartua, J.L. Pizarro, A. Grzechnik, M. Insausti, R. Kaindl, J. Sol. State Chem. 181 (2008) 1759–1766.
[17] A. Dhahri, J. Dhahri, M. Oumezzine, Mater. Lett. 63 (2009) 121–123.
[18] L. Ortega-San Martin, J.P. Chapman, E. Hernández-Bocanegra, M. Insausti, M.I. Arriortua, T. Rojo, J. Phys.: Cond. Matter 16 (2004) 3879–3888.
[19] T. Kumar Mandal, J. Gopalakrishnan, Chem. Mater. 17 (2005) 2310–2316.
[20] J. Rodríguez-Carvajal, Physica 192 (1993) 55–69.
[21] B. Ravel, M. Newville, J. Synchrotron Radiat. 12 (2005) 537.
[22] T.C. Hansen, P.F. Henry, H.E. Fischer, J. Torregrossa, P. Convert, Meas. Sci. Technol. 19 (2008) 034001.
[23] A. Faik, J.M. Igartua, J.L. Pizarro, J. Mol. Struct. 920 (2009) 196–201.
[24] M. Karppinen, H. Yamauchi, Y. Yasukawa, J. Lindn, T.S. Chan, R.S. Liu, J.M. Chen, Chem. Mater. 15 (2003) 4118.
[25] F. Bardelli, C. Meneghini, S. Mobilio, S. Ray, D.D. Sarma, Phys. Scripta 115 (2005) 475.
[26] Q. Lin, M. Greenblatt, M. Croft, J. Sol. State Chem. 178 (2005) 1356.